

# The Zwicky Transient Facility Camera

Richard Dekany, Roger M. Smith, Justin Belicki, Alexandre Delacroix, Gina Duggan, Michael Feeney, David Hale, Stephen Kaye, Jennifer Milburn, Patrick Murphy, Michael Porter, Dan Reiley, Reed Riddle, Hector Rodriguez, Eric Bellm

Caltech Optical Observatories, 1200 E. California Blvd, CA 91125, USA

## ABSTRACT

The Zwicky Transient Facility Camera (ZTFC) is a key element of the ZTF Observing System, the integrated system of optoelectromechanical instrumentation tasked to acquire the wide-field, high-cadence time-domain astronomical data at the heart of the Zwicky Transient Facility. The ZTFC consists of a compact cryostat with large vacuum window protecting a mosaic of 16 large, wafer-scale science CCDs and 4 smaller guide/focus CCDs, a sophisticated vacuum interface board which carries data as electrical signals out of the cryostat, an electromechanical window frame for securing externally inserted optical filter selections, and associated cryo-thermal/vacuum system support elements. The ZTFC provides an instantaneous  $47 \text{ deg}^2$  field of view, limited by primary mirror vignetting in its Schmidt telescope prime focus configuration. We report here on the design and performance of the ZTF CCD camera cryostat and report results from extensive Joule-Thompson cryocooler tests that may be of broad interest to the instrumentation community.

**Keywords:** CCD mosaic, cryostat, wide-field imaging, Schmidt telescope

## 1. INTRODUCTION

The Zwicky Transient Facility (ZTF) will be a significant new private/public capability for exploring the transient universe at high observing cadence [1]. Building on the existing Palomar Transient Factory (PTF) and intermediate-PTF (iPTF) infrastructure at Palomar Mountain, ZTF consists of both an Observing System (OS), previously described [2], and a significant new Data System (DS) to be described elsewhere. In this paper, we describe a key new element of the OS, the ZTF Camera (ZTFC), which is required for execution of the ambitious ZTF science program.

The ZTFC will scan large areas of the available sky several times per night to search for transient events, via near-real-time reference image subtraction. In addition to acquiring 240-300 two-color images at each location in the Northern Hemisphere per year in execution of a fast-transient survey, the full ZTF dataset will be combined to create a deep reference field of the Northern declination cap in support of source selection for DESI [3]. While all images will be sky noise limited, this initial survey can benefit from longer exposures (higher duty cycle), which will relieve the need for telescope speed upgrades to be complete prior to survey start.

ZTF prioritizes field of view over depth to bias transient event detection towards targets that are bright enough for follow-up spectroscopy, a fundamental difference and complimentary function to LSST. ZTFC is designed for 1 arcsec pixel sampling to appropriately sample the 2 (2.2) arcsec FWHM delivered image quality with Mould R-band (Sloan  $g'$ -band) optical filters.

For 30 s exposures during dark time, the limiting magnitude is expected to be 21 (21.5) in R-band ( $g'$ -band). Reducing overheads from 46 s (in PTF) to less than 15 s (10 s goal), through faster CCD readout and telescope and dome drive upgrades, allows exposure time to be reduced from 60 s to 30 s to improve frame rate by 2.7 (106 s frame time  $\rightarrow$  40 s) and duty cycle by 18% (57% duty cycle  $\rightarrow$  75%), while remaining sky noise limited (darkest sky  $> 25 \text{ e-/s/pix}$ ).

At 386 mm x 395 mm corner to corner and 89% fill factor, the ZTFC CCD mosaic has 8% greater field of view than the 14-inch photographic plates used on the same telescope during the two color Palomar Optical all Sky Survey from 1950 to 1957, POSS [4]. The fully automated ZTF will observe the same number (33,660) of square degrees as POSS to similar depth, in just 8 hours per color, revisiting the same coordinates several times per night. Images will be relayed in near real time to the Caltech's IPAC, where they will be processed and compared automatically to detect new transients within minutes of the latest observation. At a slower rate, IPAC will process fully calibrated data and house a legacy archive of all ZTF data.

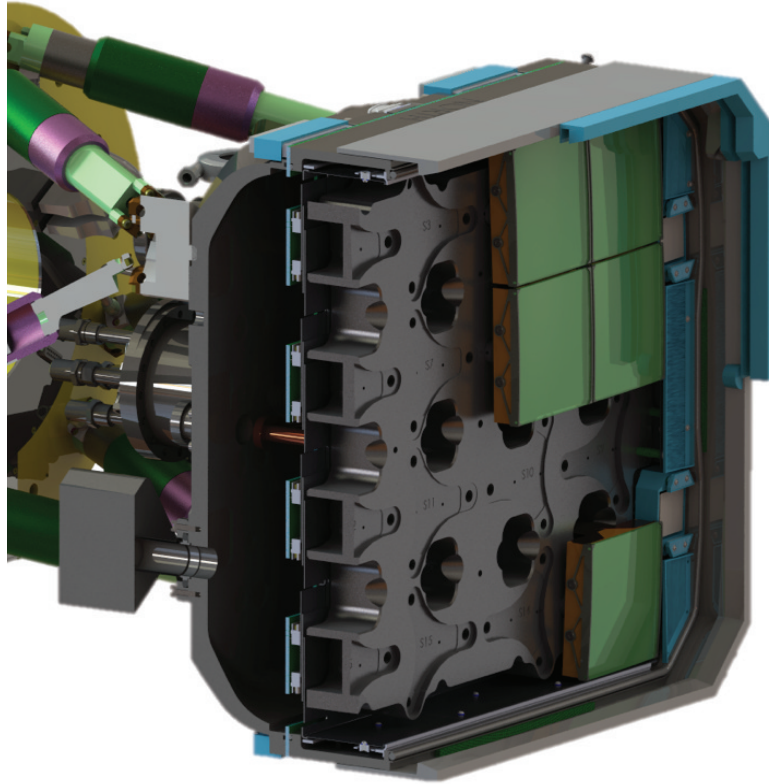


Figure 1. Cutaway solid model of the Zwicky Transient Factory (ZTF) camera. A cryocooler can be seen nestled behind the cryostat among the legs of a supporting active hexapod.

Many improvements, such as autoguiding, autofocus, active tilt and collimation, and removal of heat from the dome, are aimed at delivering 2 arcsecond image quality more consistently than for the present PTF survey. Higher CCD QE in the band-passes of interest will also enhance throughput. At nearly 400 mm square, the focal plane is quite large compared to the 1.2m diameter telescope beam which it obstructs. Therefore, a key constraint driving the mechanical design of the camera has been to minimize the telescope obscuration induced by the on-axis prime focus cryostat, filter exchange mechanism, cabling, refrigeration infrastructure, and supporting mechanical structures (as seen from all field angles.) Dewar, shutter, filter and spiders therefore, have been redesigned to limit beam obstruction to only 22.5% absolute, in spite of the large increase in field of view.

## 2. CRYOSTAT OPTICS AND MOUNTS

Because the Samuel Oschin Telescope was originally designed to expose photographic plates, its optical design does not account for the thick window required by the cryostat to maintain appropriate thermal/vacuum conditions for optimal CCD operation. The system configuration requires modification to the aspheric coefficient of the Schmidt design of the telescope<sup>2</sup>, to accommodate the large field of view and cryostat optics.

Light enters the cryostat through a 32 mm center-thickness spherical, meniscus fused silica window. Although this lens provides partial field flattening, the large physical format of the focal plane and our individual CCDs requires additional field flattening. By mounting CCDs on the flat chords of a spherical parent surface, we approximate the residual curvature of the focal plane after the powered window. Thus, the CCD mounting surfaces of the cold plate are analogous to tortoise shell topology. Finally, a plano-convex lens (convex radius 1260 mm, plano side toward CCD) is mounted 2.0 mm in front of the light-sensitive surface of each CCD, a height sufficient for safe assembly and protection of the raised CCD wire bonds.

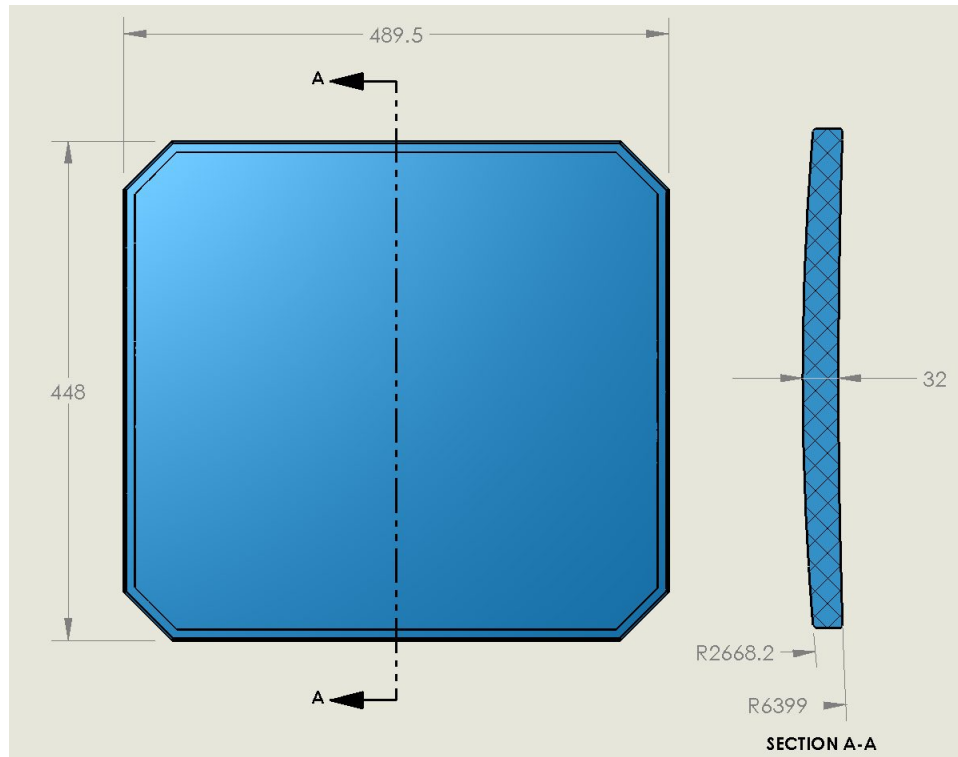


Figure 2: ZTF window as dimensioned for fabrication. The window is slightly meniscus and must support approximately 3 tons of force due to atmospheric pressure under vacuum.

## 2.1 Window Support

The window is supported by two compliant mechanisms: 1) an O-ring track around the perimeter and 2) rectangular gaskets inset from the O-ring. In addition to supplying a uniform support around the perimeter of the window, the O-ring provides the vacuum seal between the stainless steel instrument enclosure and the fused silica glass. The rectangular gaskets are an additional means of supporting the window and, the larger of the two pairs, supplies voltage to an electrically resistive but optically transmissive ITO coating incorporated in the anti-reflection coatings on the inner surface of the window to maintain temperature at ambient by replacing the ~30 W radiated into the cold interior. The durometer and geometry of the supports were optimized to reduce the stress on the window. As seen in Figure 3, the available location of the O-ring and support gaskets was limited by the shape of the instrument enclosure and the field of view of the CCDs. The supports are located as close to the center of the window as possible without encroaching the on the field of view of the CCDs. Outside of vacuum, the window is encapsulated in an Ultem 9085 3D-printed frame which constrains the glass from shifting laterally relative to the rest of the instrument and captures the glass vertically in the event of vacuum loss and protects the window edges from accidental impacts.

Finite element analysis of the slightly meniscus window predicts a factor of safety equal to seven. To achieve this figure the area of supplemental gaskets was adjusted to provide additional supporting forces in the middle of the sides such that bending along the edges is eliminated. As strain is reduced so too is stress. FEA shows that the resulting stress distribution is less centrally concentrated, extending more along the diagonals, resulting in lower peak stress at the center. Vertical faces at the edge of the window have been polished to prevent crack initiation there. Careful visual inspection for small chips and crack, then vacuum test without CCDs installed will be employed to test for infant mortality. Over-pressure testing will not be performed since this will only hastens ageing (crack propagation) without providing any guarantee against future failure.

## 2.1 Field flatteners and frames

The 16 field flattener lenses (one per CCD) are held between pairs of 3-D printed titanium frames, black anodized, attaching and registering to each of the two sides of each CCD package as shown in Figure 4. These frames perform several important functions. They accurately hold each field flattener above the CCD by referencing the sides of the CCD package, and thermally isolate the lens from the CCD through thin struts design. In addition to their optical function, field flattener lenses mechanically protect the CCD and bond wires. Beyond the image area, the inner surface is screen printed with black epoxy ink to prevent light from scattering off the bond wires.

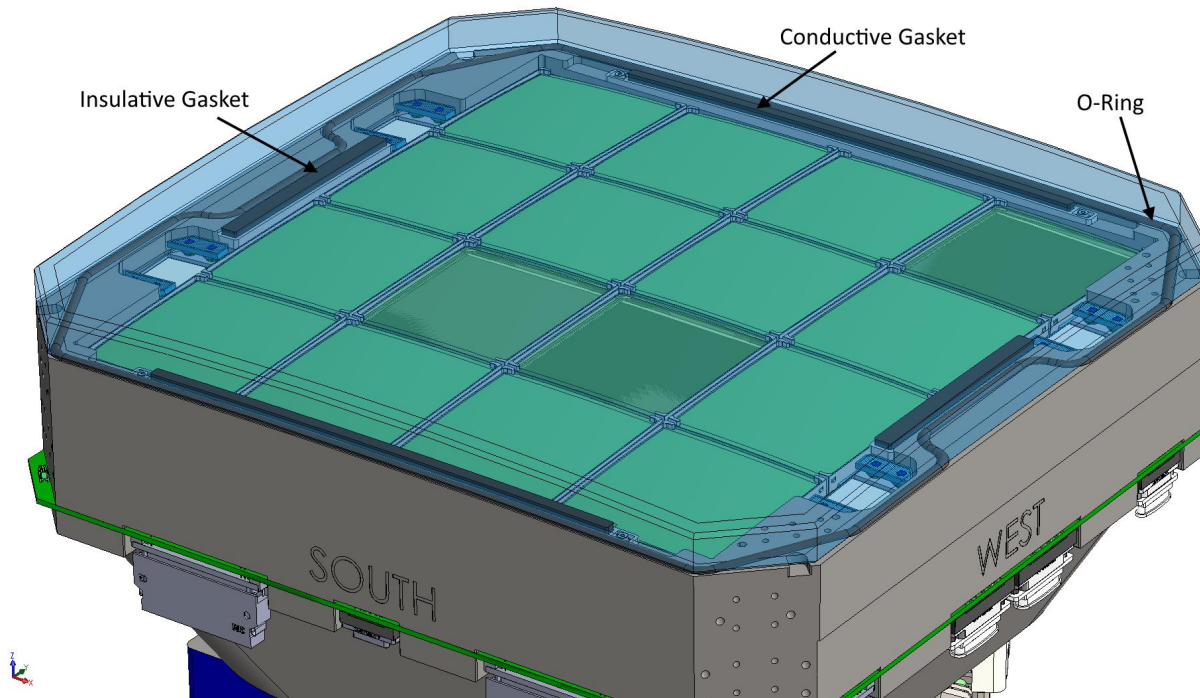


Figure 3: ZTF window gasket and O-ring layout. The dewar window is supported by double O-rings at the edge of the optical beam and will be surrounded by a thin frame which must be compliant enough to protect it from impact yet strong enough to support the window in the event that the vacuum is released. Given that the frame must wrap around the spherical shape of the window a 3D printed part made from carbon-filled nylon is under consideration. We have had good experience supporting mirrors in the past with printed parts made by solidconcepts.com from NyTek1200 by Selective Laser Sintering.

The field flattener lens mount design provides a nominal clearance between the lens and frames at operating temperature to accommodate material coefficient of thermal expansion differences and manufacturing tolerances without overstressing the lens. Clearance is a minimum of 0.100 mm at operating temperature.

The frames are made of Ti-6Al-4V Titanium, manufactured by GPI Prototype using the Direct Metal Laser Sintering (DMLS). DMLS is an additive (3D printing), process in which a layer of metal powder is melted via laser light and cools in place. While initially we were concerned with internal-stress-related warping upon cooling [1], experiments showed this to be a non-issue. The finely stippled surface produced by the DMLS process is a black anodized by Techmetal, Inc. using their Techcoat DLA200™ process.

The lens is constrained axially between two small tabs protruding at each corner with the gap being custom fitted to the corner thickness of each Field Flattener, for the most part by matching up the dimensional variations of the lenses with those of the frames, and filing some frames where necessary. Storage trays have been fabricated to allow this pairing to

be maintained thru assembly and dis-assembly. The Field Flattener Frames and lenses protect the bond wires at the corners the CCDs during mosaic assemble, once the CCD and lenses have been mated.

Thin struts between the lens contact points and the attachment to the side of the CCD package, and the low conductivity of titanium, provide thermal isolation, see Figure 5.

Registration with the SiC CCD package is defined by 3 tabs. Frames are attached to the CCD with screws which thread into a set of "nut plates" embedded into the CCDs. Flexures incorporated into the nut plate maintain tension on the screw and accommodate thermal contraction, pinned on the side of the registration tab where the fastener is torqued down first and slipping on the other side, where a lower torque is employed. While the spring action of the nut plate may be sufficient to prevent unscrewing due to thermal walk, a small dot of epoxy between the screw head and the frame is provided as an additional precaution.

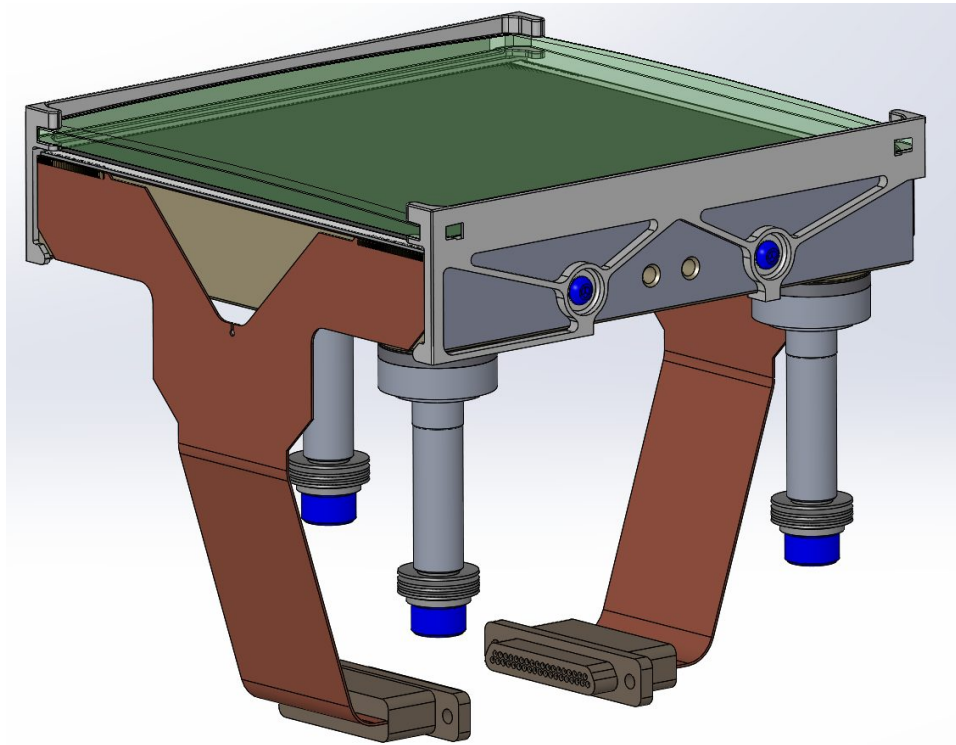


Figure 4: CCD with the Field Flattener held by the Titanium Frames.

The combination of poor thermal contact to the field flatteners and low conductance of the thin titanium steel struts allows the field flattener temperature to be governed by radiative equilibrium so field flatteners function as a floating radiation shields. This provides almost a factor-of-two cooling power margin for the cryostat design, using just two Polycold Compact Coolers charged with PT16 refrigerant. The four high-pressure refrigerant lines, connecting to independent compressors, are hidden within the 3<sup>rd</sup> spider vane.

Along two edges of the CCD, the silicon has been etched away by e2v to expose the front-surface metal for wire bonding. These two edges are the only areas of the CCD which is not AR coated. To prevent reflections from both the bond wires and the uncoated edge, the CCD facing edges of the field flattener will be painted black (and vacuum baked to eliminate outgassing). Fortunately the AR coating extends beyond the image area further than the 800  $\mu\text{m}$  beam footprint so it is possible to full obscure the reflective areas without the penumbral zone extending into the image area. The CCD is AR coated to the edge on the sides where the field flatteners enter into a pocket in the frames, so no paint is applied to these edges eliminating the risk of paint scarping off and getting onto the CCD surface.

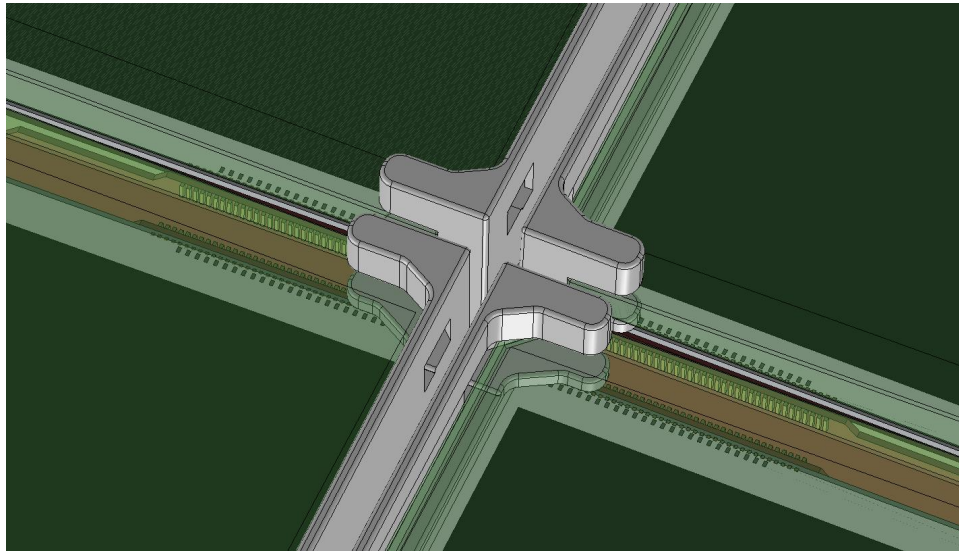


Figure 5: The enlarged view of a corner where 4 CCD come into close proximity is shown to reveal the 2 mm clearance over the bond pads. The frames and lenses prevent contact with the CCD itself.

### 3. CRYOSTAT MECHANICAL DESIGN

#### 3.1 Overview

The cryostat and its support system are designed to perform two fundamental functions. First they must maintain the position of the ZTF CCDs relative to the curved image plane of the Samuel Oschin Telescope to within an allocated tolerance related to the seeing-limited depth of focus of the telescope beam, and do so in all telescope orientations. Second, the cryostat design must also successfully allow for the cooling of the focal plane and maintenance of the CCD operating temperature of approximately 160K, in vacuum to avoid condensing contamination of the detectors.

The dewar width is reduced towards the rear so that it remains hidden behind the window even when viewed off-axis. To achieve 20% obstruction, the window extends only two O-ring thicknesses beyond the converging beam, and the window frame only extends a few millimeters beyond that. Beam obstruction is increased by ~2% by the inclusion of 2Kx2K guide and focus CCDs along two edges of the focal plane, but this loss of throughput is expected to be more than compensated by improvement in delivered image quality made possible by the these sensors.

#### 3.2 CCD Cold Plate Mount to the Sidewalls

Three titanium bipods located at two corners and at the middle of the opposing side attach the CCD cold plate to the sidewall as shown in Figure 8. These bipods perform several functions:

- Thermally isolate the CCD Cold Plate Mount (163K) from the Side Wall (~285K).
- Control height and tilt, and lateral XY position in any required gravity orientation. (40um Max shift with E-W pointing down)
- Keep resonant frequency well above power spectrum of disturbances such as shutter motion and wind buffeting.

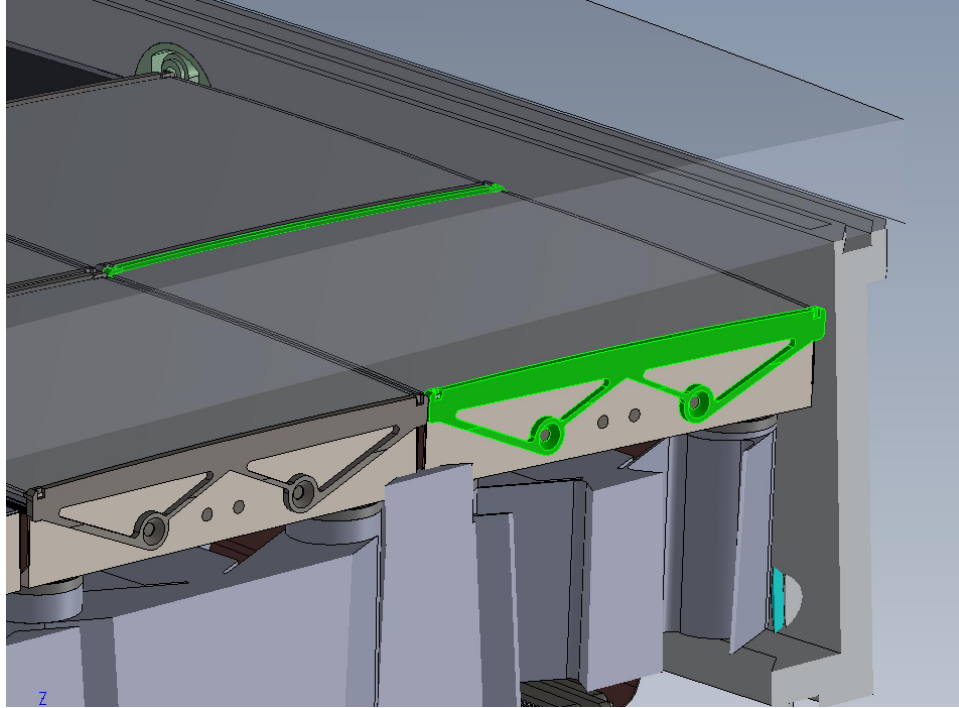


Figure 6: Cross section cutting between edges of science focal plane and guide CCD to reveal field flattener frames. (corner CCD highlighted in green).

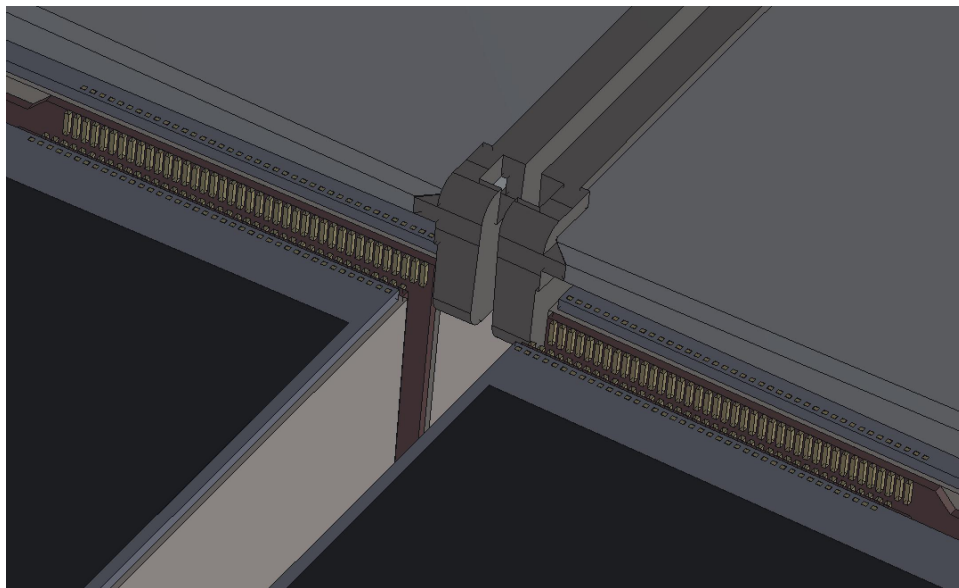


Figure 7: The enlarged view of a corner where 4 CCD come into close proximity is shown with field flatteners removed from CCDs nearest the viewer to reveal the 2 mm clearance over the bond pads. The frames and lenses prevent contact with the CCD itself.

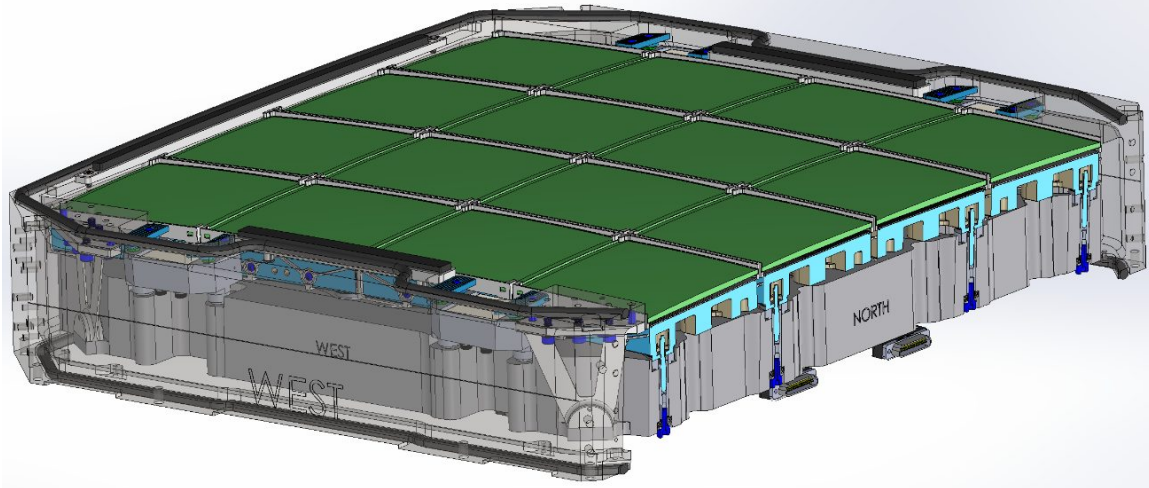


Figure 8. ZTF cold plate interface.

### 3.3 CCD Installation to the Cold Plate

Relative CCD positioning on the cold plate is critical to achieving appropriate image quality. Our positioning strategy calls for the CCD studs themselves to be attached to the cold plate by tube fasteners, allowing more precise height control than flexures accommodating lateral controlled slippage to accommodate thermal contraction.

The position of the CCD on the cold plate is thus achieved by a single fastener fitting tight with one of the cold plate hole, constraining horizontal translations. Orientation is controlled using a slot interfacing with the second precise fastener, constraining rotation about the positioning fastener. The last fastener is a loose fit, constraining the last degrees of freedom. Each CCD tip, tilt and height is controlled by three precision ground spacers inserted between the e2v resting pad and the cold plate.

The attachment of the CCD to the cold plate is controlled by limiting the force in the studs per e2v recommendation, using a suitable stack of spring washer. The expected stud force is 56 lbf so assuming a coefficient of friction of 0.2, the maximum shear force prior to slippage will be 13 lbf, which is acceptable, based on FEA evaluating stress in the SiC CCD package.

CCDs are installed onto the cold plate using tapered handling rods reaching the CCD e2v provided threaded studs, through the cold plate guiding the CCD to the focal plane. The handling rods are then successively replaced with the custom CCD fasteners.

## 4. CCDS AND ELECTRONICS

### 4.1 e2v Science CCD231-C6

CCD manufacturers have reduced defect density to the point where lowest cost per unit area is achieved with the largest CCD that fits on a 150 mm silicon wafer. In 2012 ZTF executed a competitive bid process for the sixteen 6144x6160 pixel CCDs required to completely tile a 47 deg<sup>2</sup> instantaneous field of view, selecting e2v, Inc. in February 2013. The anticipated high yield has been confirmed by the delivery of the first batch of six CCD231-C6s within 9 months after placement of the order. These met all specifications, and exceeded them in key areas such as height, flatness, QE, and cosmetic defects.

Fortuitously, the standard 15 $\mu$ m pixel size maps to 1 arcsec providing Nyquist sampling of the anticipated 2 arcsec delivered image quality. This image sampling matches that of PTF, providing adequate spatial sampling while minimizing the number of pixels to be digitized, stored and processed. By sampling the PSF no more finely than Nyquist, not only is the number of pixels minimized but signal per pixel is maximized, relaxing read noise requirement so that pixel rate can be higher. Substantial cost savings are then realized by meeting the 10s readout goal with only four

outputs per CCD. The single-ended read noise measured by e2v at 500kHz for the 24 output amplifiers delivered so far shows a tight distribution: allowing  $\sqrt{2}$  noise increase for differential outputs and another  $\sqrt{2}$  for 1MHz operation, the mean read noise is projected to be 11.1e- with 0.3 e- standard deviation. This degrades total noise by 9% for 30s exposures in darkest sky conditions.

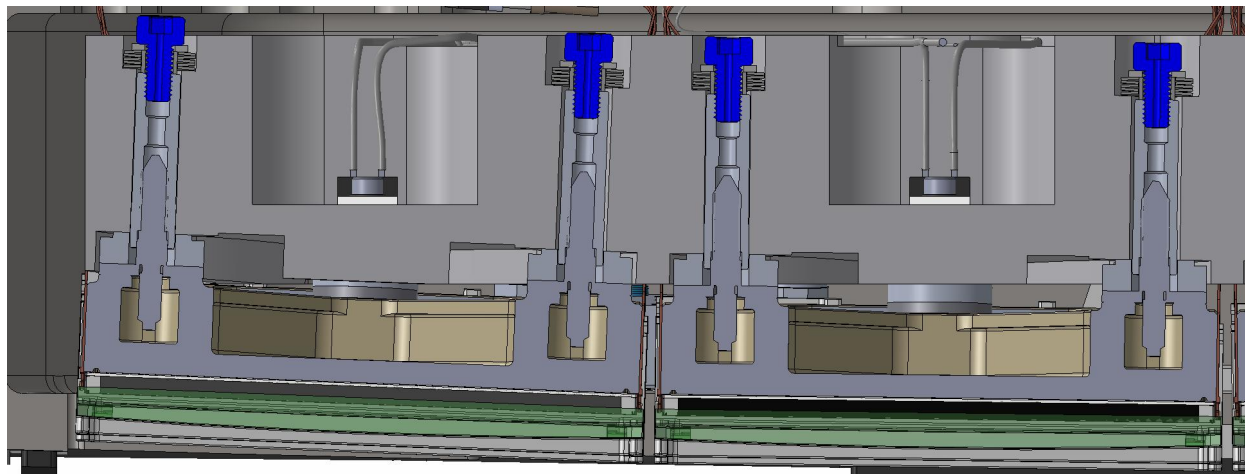


Figure 9. Cross section of the cold plate showing the CCD fastener tube design.

The only customization of the CCD231-C6 is the single layer AR coating thickness. QE averaged over all pixels received to date is 82% at 400 nm rising to 97% at 500 nm and falling only to 80% at 700nm. Improvements at the band edges may be obtained on the remaining CCDs by employing some variant of the multilayer coating which e2v is applying to identically sized CCD290-99s on JPAS [5].

The coarse image scale requires a CCD with the lowest possible lateral charge diffusion to minimize this contribution to PSF degradation. Since ZTF has no requirement for extended red response, a CCD with conventional thickness and resistivity could be selected. Not only does this improve yield and thus lower the cost, but also has the benefit that lateral charge diffusion can be reduced to 0.65 pixel FWHM in g' band and 0.45 pixel in R, merely by operating with positively biased image-area clocks to minimize undepleted thickness[6].

#### 4.2 Guide and Focus CCDs

A single 2Kx2K guide CCD will be installed just outside of, and parfocal to, the science CCD mosaic. This fully depleted n-channel CCD was design by Semiconductor Technology Associates, manufactured by Dalsa and delta-doped and AR coated and packaged by the Micro Devices Laboratory at JPL. The custom package allows for close butting of these focus and guide CCDs along two edges of the science focal plane to squeeze the guiders into the optically corrected field and minimize the growth in instrument size saving a few percent in beam obstruction compared to commercial devices. Thus, this CCD has extended spectral response to both the blue and red, resulting in excellent guide star sensitivity.

The guide CCD will operate in full frame mode and read out while the telescope shutter is open. Since guide stars are bright, we will use 1MHz pixel rate without sacrifice of guiding performance. With split frame readout, readout of all pixels requires two seconds. It is anticipated that after an initial 2 sec exposure and 2 sec full frame readout, a smaller region of interest will be automatically selected, at which point the image smear time will drop to tens of milliseconds. Exposure time can remain at 2 s to integrate the seeing, but smear time will drop to 1%. At the same time that a region of interest is selected, the pixel rate will be reduced to bring read noise below sky noise.

Three 2Kx2K out-of-focus CCDs, identical to the guide CCD, are located symmetrically around the science mosaic with respect to the guide CCD, but have a focus offset of 1.45 mm (upstream, so preceding telescope focus.) These prefocal images will be used to maintain cryostat hexapod focus, and cryostat tip and tilt degrees of freedom. The extra-focal

imaging method pioneered by Tokovinin [7] (CTIO) and refined for DES and LSST by Roodman[8] (SLAC) will be used for measuring the low-order Zernike coefficients of the wavefront errors. The focus term at three corners provides an accurate measure of piston/tip/tilt with little sensitivity to image seeing, which is monitored by the 4<sup>th</sup> (guider) CCD. As for DES and LSST, analysis of the intensity distribution across the defocused image will also provide a measurement of higher order wavefront errors that can be diagnostic various misalignment or mirror support problems[9]. Extra-focal-imaging CCDs share the science shutter so exposures are concurrent. Readout is pixel and line-synchronous with the science CCDs, but completes in 1/3rd the time, so that with sufficiently fast analysis the hexapod could be repositioned before the following exposure.

The guide and focus CCDs are configured to read from one amplifier per serial register, this allows the amplifier at the other end to be used the reference side of a differential pair. One can still select the nearest amplifier, so little functionality is lost. As for the science channels, differential readout is expected to strongly attenuate clock feedthrough transients enabling faster pixel rate and reducing line start transient (typically a consequence of serial clock feedthrough), at the cost of root-two read noise increase. Since readout time is dominated by parallel for region-of-interest readout, the noise penalty for differential transmission can be mitigated by approximately doubling the pixel time, without significant loss of frame rate.

### 4.3 CCD controllers

ZTF detectors will be controlled using a group of Semiconductor Technology Associates (STA) “Archon” controllers [10] that drive 4 CCDs from each of 5 chassis (4 science and 1 guide/focus chassis). To minimize the cost and complexity of the electronics a single controller operates each quadrant of the mosaic. Readout will be strictly pixel synchronous to avoid patterns in the images caused by clock-to-video crosstalk: all controllers share a common master clock, execute identical code and will be triggered by a common signal. The clocks for four CCDs are ganged together so that each quadrant appears to be a single 16 channel CCD. The ganging of the same parallel clock across 4 CCDs leads to ~275  $\mu$ s minimum parallel shift time, given the 250 mA clock drive capability, and thus 0.85s for the 3080 parallel shifts per frame. Each serial clock driver is connected to the same pin on pairs of CCDs to provide 44ns worst-case transition time. Given the requirement for three coincident transitions, 1 MHz pixel rate is easily supported.

The CCD electronics will be located outside telescope tube to avoid obstructing the beam. The STA controller circuit boards are cooled via conduction to water-cooled heat sinks within each chassis. Cooling water will be refrigerated to approximately ambient to avoid both condensation and the need for anti-freeze, which can be corrosive.

### 4.4 Vacuum Interface Board (VIB)

A major simplification to the dewar wiring is provided by the “Vacuum Interface Board” (VIB). This alternative to hermetic connectors was pioneered in small CCD cameras by Mackay[11], and scaled successfully to 14”x22” by Atwood[12]. The VIB is trapped between O-rings in the sidewall and rear cover as shown in Figure 11. ZTF’s VIB is a 0.125” thick multilayer printed circuit board, which, at 19.1” x 17.4”, fits within the common 24”x18” size limit for many vendors. While bare resin finish has been shown to make a good seal on other VIBs, gold plated copper is contemplated for lower emissivity, with the secondary benefit of lower outgassing. 1408 total signals from all 20 CCDs are routed from the CCD connectors on internal layers around cut-outs for access to CCD fasteners and flex cables. All cables and connectors were made by 3-M and Glenair.

The current instrument-mounting hub provides only focus motion, suffers from backlash and may not be strong enough to carry ZTF as it was only designed for the photographic plate holder. The present focus hub is supported by four solid spiders with uniform cross-section with no provision to hide the cables or compressed refrigerant hoses. These will be replaced by new spiders, which are each split into top and bottom sections with a space for cables in between (at the widest point). The vanes have triangular cross section, tapering towards the outer edges so that their beam obstruction is almost independent of field angle. Profiling of their surface reduces scattered light. Adopting three spiders instead of four reduces the beam obstruction. Diffracted power is also reduced and distributed into 6 spikes in the image instead of four. In combination, these effects will reduce the extent of diffraction around bright stars is reduced by a factor of two.

The vacuum interface board (VIB) is a 1/8” thick printed circuit board which carries the CCD signals from inside the cryostat to the outside where they can then be connected to the readout electronics. This eliminates the need for hermetic connectors in the system. As shown in Figure 12 Vacuum Interface Board in System, the VIB is mounted between the focal plane and the back plate. Two O-rings on either side of the board provide a seal for the cryostat. There are cutouts in the VIB at each CCD location to provide access to the three fasteners for each CCD.

Small profile connectors are used to minimize the beam obstruction due to the VIB. Off the shelf cables connect the signals to the readout and control electronics mounted on the outside of the telescope tube. The VIB is divided into quadrants of 4 CCDs, and each quadrant is connected to a single controller. A fifth controller interfaces with the four remaining CCDs which provide the guiding and focus information.

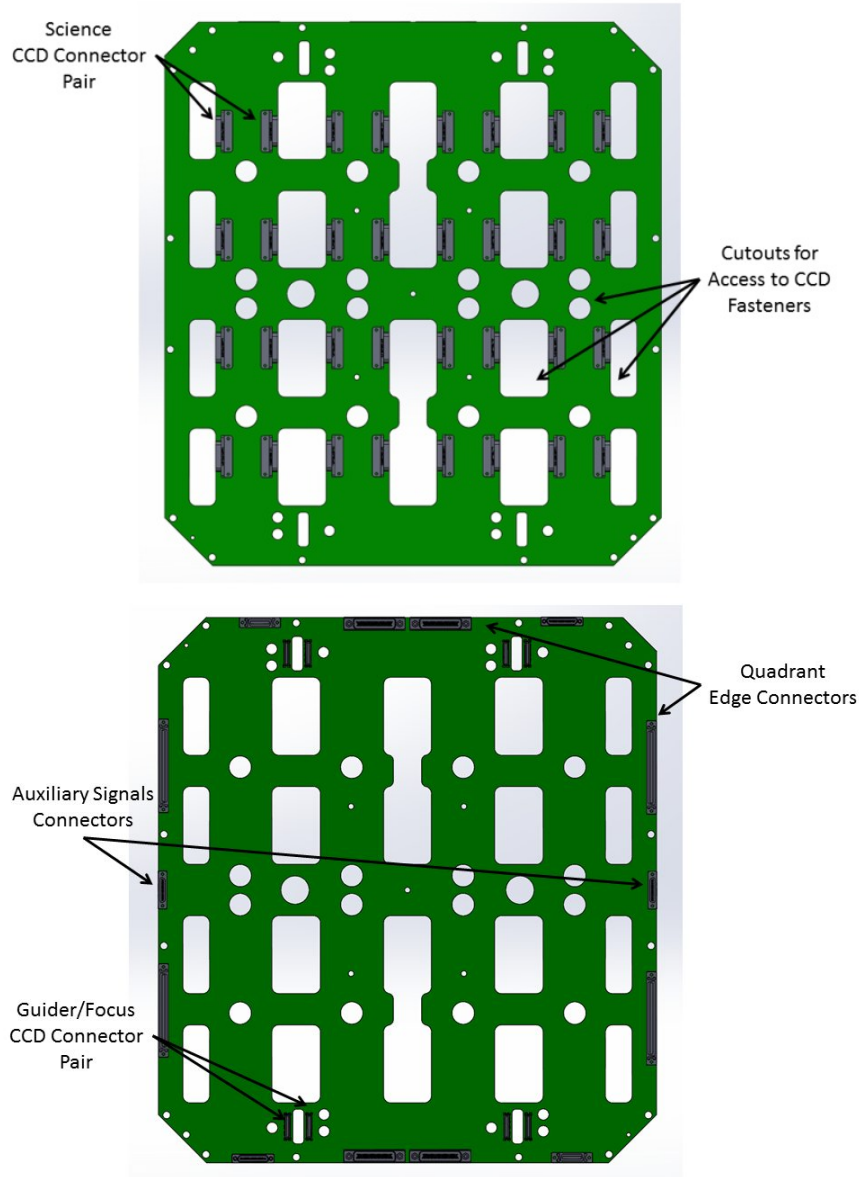


Figure 10 Focal Plane Side View of VIB (left) and Back Plate Side View of VIB (right).

Due to the long path for the video signals to the controllers, the video signal is amplified. The VIB has amplifiers for each CCD output in the mosaic – 72 channels in all. A differential design is used which subtracts the CCD signal from the dummy signal the device provides. The signal subtraction increases the noise by a factor of  $\sqrt{2}$ , but reduces common mode noise from clock and bias signals. The differential signal also reduces susceptibility and interference from other channels which eliminate the need for crosstalk subtraction for the mosaic.

In addition to the CCD signals, the VIB also routes signals for thermal management and filter mounting sensors. Two auxiliary signal connectors provide signals for 20 thermal sensors, 5 heaters, high voltage for the window heater, and positive latching signals for the various filters mounted to the front of the cryostat window.

## 5. ILLUMINATOR

Laboratory testing prior to receipt of the cryostat window is facilitated through the use of a surrogate cryostat cover, designed to maintain internal vacuum and provide built-in illumination sources. This cryostat cover also provides a dry environment for the window, which operates below ambient temperature during normal operations and could otherwise condense or frost during testing.

The illuminator can be used with or without a window and can act in a similar fashion as the Vacuum Interface Board creating a vacuum seal and carrying the electrical signals out of vacuum when no window is present. The board has a gold coating on the surface facing the focal plane for a low emissivity. There is a matrix of 272 LEDs (831nm) that are grouped in a 12x8 matrix allowing for multiple patterns to illuminate the CCDs as shown in Figure 13. In addition to the LEDs, there are 5 portholes on the board that can be used to focus light onto each of the guide and focus CCDs and the middle of the science focal plane. LED intensity can be modulated using digital-to-analog converters on the board and are controlled by an Arduino microcontroller.

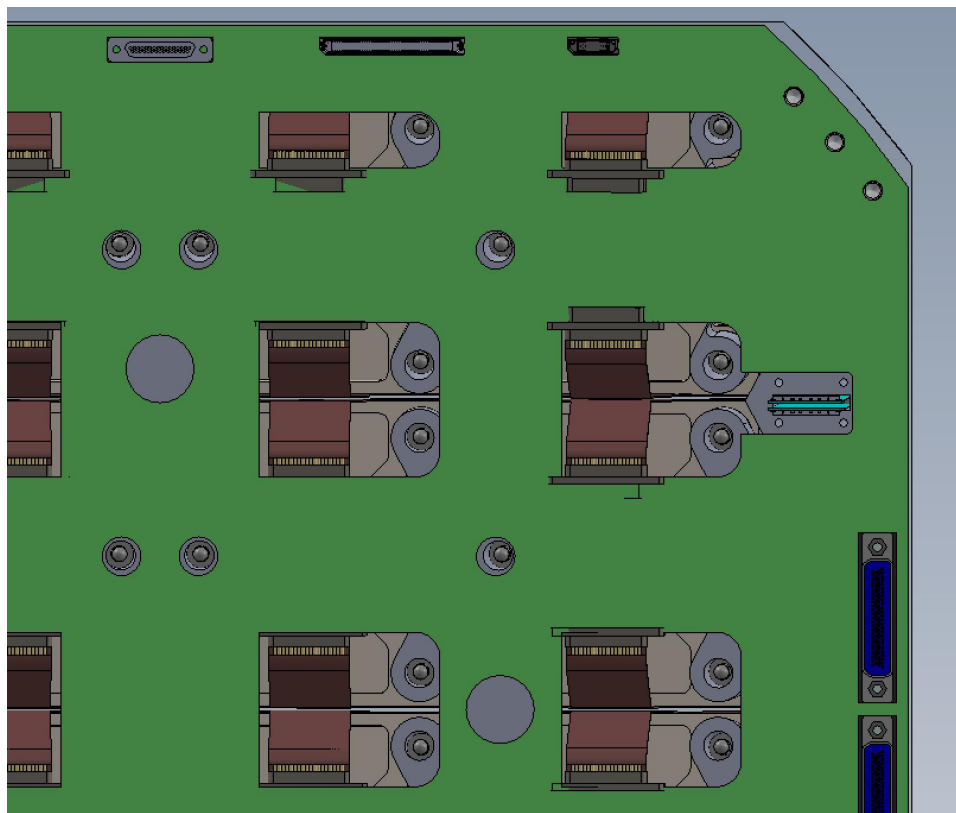


Figure 11: View of one quadrant of VIB with rear cover to reveal cut outs for accessing CCD retention hardware and flex cables from CCDs. These engage with connectors in the VIB inserting parallel to the VIB (sideways) on the CCD side (concealed in this view). Preamplifiers (not shown) will be located close to the connectors and will be cooled conductively through copper ground and power planes. Signals will be routed on internal layers of the VIB to connectors to COTS cables located around the perimeter.

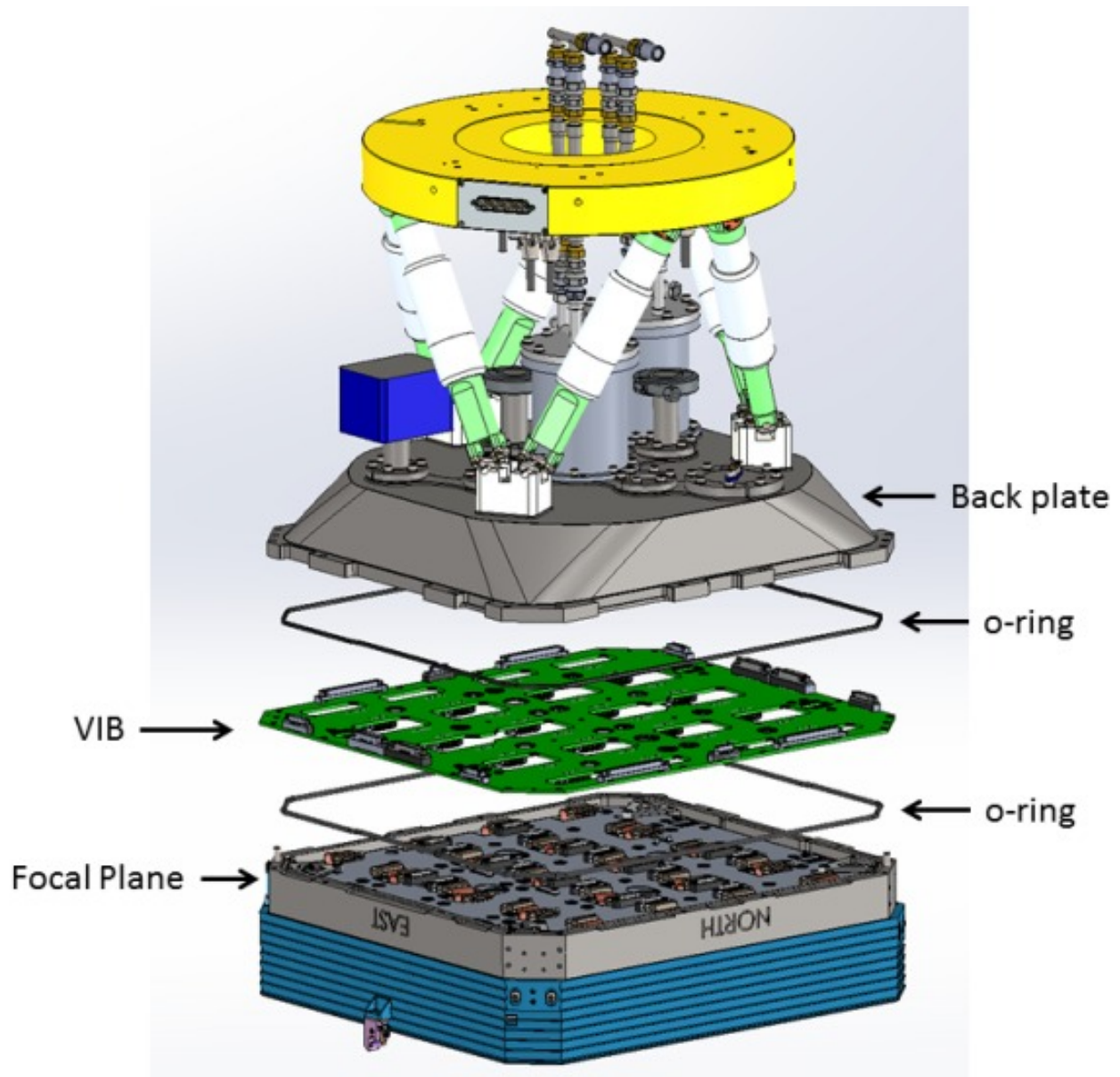


Figure 12 Vacuum Interface Board in System. CCD signals are routed from the internal connectors for each device to small profile connectors on the edge of the VIB.

## 6. ACKNOWLEDGMENTS

ZTF is enabled by a private/public partnership, with major support from the National Science Foundation Mid-Scale Instrumentation Program (MSIP). Private partner participation includes major commitments from California Institute of Technology, USA; University of Maryland, USA; University of Wisconsin-Milwaukee, Weizmann Institute for Science, Israel; Oskar Klein Centre at University of Stockholm, Sweden; and Humboldt University, Germany.

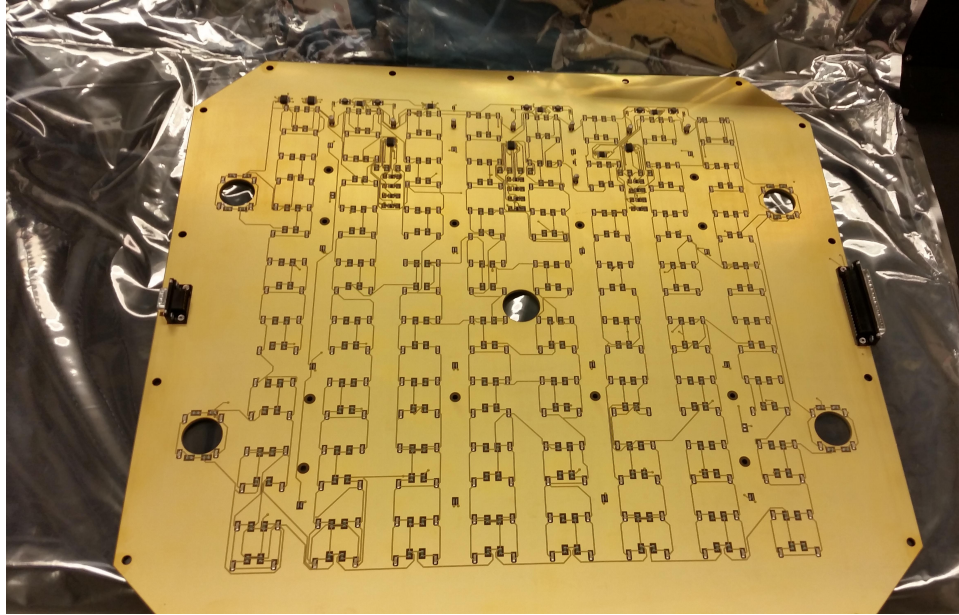


Figure 13. As-built view of the ZTF cryostat illuminator.

## REFERENCES

- [1] Smith, R., Dekany, R., Bebek, C., Bellm, E., Bui, K., Cromer, J., Gardner, P., Hoff, M., Kaye, S., Kulkarni, S., Lambert, A., Levy, M., and Reiley, D., "The Zwicky Transient Facility Observing System," Proc. SPIE 9147, 914779-1, (2014).
- [2] Law, N., Kulkarni, S., Dekany, R., "The Palomar Transient Factory: System Overview, Performance, and First Results," PASP, 121, 1395L (2009).
- [3] Levi, M., Bebek, C., Beers, T., Blum, R., Cahn, R., Eisenstein, D., Flaugh, B., Honscheid, K., Kron, R., Lahav, O., McDonald, P., Roe, N., Schlegel, D., representing the DESI collaboration, "The DESI Experiment: a white paper for Snowmass 2013," eprint arXiv:1308.0847.
- [4] Minkowski, R. L., & Abell, G. O., [Stars and Stellar Systems, Vol. 3], Basic Astronomical Data, ed. K. A. Strand, Chicago University Press, 481 (1963).
- [5] Harris, R. D., Jorden, P. R., Bastable, M., Pike, A., Dryer, M., Pittock, R., Marin-Fanch, A., Taylor, K., Palmer, I., Wheeler, P., Renshaw, R., Fenimore-Jones, G., Taylor, A., Haddow, G., Swindels, I., Barwick, M., "A gigapixel cryogenic focal plane array camera for JPAS 2.5 m survey telescope," Proc. SPIE 9154, 915428 (2014).
- [6] Downing, M., Baade, D., Deiries, S., Jorden, P., "Bulk Silicon CCDs, Point Spread Functions, and Photon Transfer Curves: CCD Testing Activities at ESO" Detectors for Astronomy, (2009).  
<http://www.eso.org/sci/meetings/2009/dfa2009/program.html>
- [7] Tokovinin, A., Heathcote, S., "Donut: measuring optical aberrations from a single extra-focal image," PASP Vol. 118, No. 846. 1165-1175 (August 2006). [doi:10.1086/506972](https://doi.org/10.1086/506972)
- [8] Roodman, A. J., Riel, K. A., Davis, C., "Wavefront sensing and the active optics system of the dark energy camera," Proc. SPIE 9145, 914541 (2014).
- [9] Schechter, P. L., Sobel Levinson, R., "Generic misalignment aberration patterns and the subspace of benign misalignment," Proc. SPIE 8444, 844455 (2012). [http://dx.doi.org/10.1117/12.925075](https://doi.org/10.1117/12.925075)
- [10] Bredthauer, G., "Archon: A modern controller for high performance astronomical CCDs," Proc. SPIE 9147, 9147202 (2014).
- [11] Mackay, C., Crass, J., King, D., "Diffraction Limited Imaging from the Largest Ground-Based Telescopes in the Visible," Proc. SDW2013 (2013).
- [12] Atwood, B., Jorden, P., "The KMTNet 340 Megapixel focal planes," Proc. SDW2013 (2013).